Coralline algal Mg-O bond strength as a marine pCO_2 proxy

Maren Pauly[1], Nicholas A. Kamenos[2]*, Penelope Donohue[2], and Ellsworth LeDrew[1]
[1]Department of Geography & Environmental Management, University of Waterloo, Waterloo, Ontario N2L 3G1, Canada
[2]School of Geographical and Earth Sciences, University of Glasgow, Glasgow G12 8QQ, Scotland

ABSTRACT

Past ocean acidification recorded in the geological record facilitates the understanding of rates and influences of contemporary pCO_2 enrichment. Most pH reconstructions are made using boron, however there is some uncertainty associated with vital effects and isotopic fractionation. Here we present a new structural proxy for carbonate chemistry; Mg-O bond strength in coralline algae. Coralline algae were incubated in control (380 µatm pCO_2), moderate (750 µatm pCO_2), and high (1000 µatm pCO_2) acidification conditions for 24 months. Raman spectroscopy was used to determine skeletal Mg-O bond strength. There was a positive linear relationship between pCO_2 concentration and bond strength mediated by positional disorder in the calcite lattice when accounting for seasonal temperature. The structural preservation of the carbonate chemistry system in coralline algal high-Mg calcite represents an alternative approach to reconstructing marine carbonate chemistry. Significantly, it also provides an important mechanism for reconstructing historic atmospheric CO_2 concentrations.

INTRODUCTION

Atmospheric CO_2 concentrations have increased from 275 µatm in A.D. 1700 (Keeling and Whorf, 1999) to 400 µatm today (Tans, 2014) with the oceans absorbing 25%–30% of the CO_2 released into the atmosphere (Bates et al., 2012). The dissolved CO_2 reacts with water to form carbonic acid, and as CO_2 levels increase at the atmosphere-ocean interface, the carbonic acid is reduced to H^+ and HCO_3^-. This secondary process reduces carbonate saturation states and pH, a process called ocean acidification (OA) (Doney et al., 2009).

Such changes in carbonate saturation states can impact the marine biosphere. As the carbonate system changes, increased HCO_3^- enables calcification to continue; however, calcifiers will be prone to dissolution and metabolic disruptions (Roleda et al., 2012). Although many marine organisms are expected to be adversely affected by OA (Hall-Spencer et al., 2008b; Kuffner et al., 2007; Ries et al., 2009), interspecies variability in susceptibility exists (Fabricius et al., 2011; Inoue et al., 2013). Poorly understood organismal tradeoffs to survive OA mean new approaches are now required to understand sensitivities (Dupont and Portner, 2013; Hall-Spencer et al., 2008a).

During the Paleocene-Eocene Thermal Maximum (PETM) large quantities of carbon dissolved into the oceans causing OA, and while current anthropogenically driven CO_2 release is projected to be of similar magnitude, it will be at a higher rate than during the PETM (Zachos et al., 2005). Thus such paleoclimate events can also be used to assess rates and influences of acidification change in recent centuries.

High-resolution reconstructions of oceanic pH or pCO_2 are used to understand changes in the carbon cycle, including OA (Honisch et al., 2012). Boron has been used to reconstruct seawater pH patterns from marine carbonates, with the role of $\delta^{11}B$ as a pH proxy validated with interlaboratory calibrations (Foster et al., 2013). For example, boron isotopes have been used to reconstruct OA during the PETM (Penman et al., 2014), the Miocene Climatic Optimum (Foster et al., 2012), and the last deglaciation (Henehan et al., 2013). Uncertainty associated with proxy-derived vital effects and isotopic fractionation requires further refining to reduce propagation errors (Babila et al., 2014).

Red coralline algae are high-resolution paleoenvironmental proxies with wide geographical distribution (Henrich et al., 1995), long lifespan (Foster, 2001), seasonal growth banding (Adey and McKibbin, 1970; Foster, 2001), and, in several species, reduced structural and physiological susceptibility to changes in carbonate chemistry (Burdett, 2014; Kamenos et al., 2013; Martin et al., 2013; McCoy and Ragazzola, 2014; Nash et al., 2013). In *Lithothamnion glaciale*, a high-latitude species, there is a response of Mg-O bond strength to marine carbonate chemistry within the algal skeleton driven by the rate of pH reduction (Kamenos et al., 2013). The dependency of crystal lattice integrity on carbonate chemistry variability indicates the potential for Mg-O bond strength to act as a carbonate chemistry proxy.

In this study, we investigate the application of coralline algal skeletal Mg-O bond strength as a carbonate chemistry proxy. It is expected that (1) individuals will show seasonal patterns in Mg composition, (2) moderate and high OA treatments (high pCO_2, low pH) will alter coralline algal structural integrity, altering their Mg-O bond strength, and (3) a relationship exists between Mg-O bond strength and carbonate chemistry.

*E-mail: nick.kamenos@glasgow.ac.uk

METHODS

Lithothamnion glaciale (Fig. 1) from Scotland (Fig. 2) were cultured for 2 yr at 380, 750, and 1000 µatm pCO_2 following ambient temperature and light. Full carbonate chemistry of each treatment was calculated. Mg concentrations and Mg-O bond strength of the high-Mg calcite skeleton deposited prior to and during the experiment (n = 5 thalli per treatment) were determined using Raman spectroscopy (spot size = 15 µm). Relative Mg concentrations were determined from the position of the ~1089 cm^{-1} Raman shift peak. Mg-O bond strength was determined from the full width at half peak maximum (FWHM) of the ~1089 cm^{-1} peak (Bischoff et al., 1985; Kamenos et al., 2013). In *L. glaciale*, Mg is a component of the crystal lattice (Kamenos et al., 2009), and thus increases in Mg-O bond strength can be attributed to increasing positional disorder of crystal lattice bringing Mg and O closer together via Mg ions moving out of the plane parallel to the *a*-axis

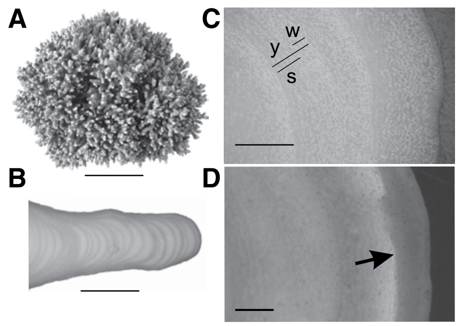

Figure 1. A–D: *Lithothaminon glaciale* thallus (A; scale bar = 30 mm) with annual (B; scale bar = 1 mm) and seasonal growth bands (C; scale bar = 200 µm); annual (y), summer (s), and winter (w) growth are shown in C. D: Fluorescent calcein stain on representative thallus (arrow) (scale bar = 200 µm).

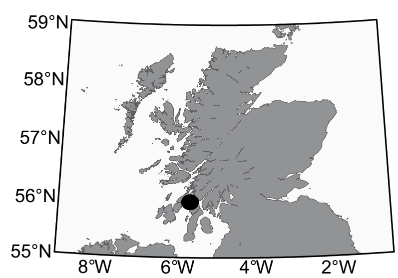

Figure 2. Scotland, with the sampling location (black dot). Map generated in Ocean Data View software (http://odv.awi.de).

GEOLOGY, March 2015; v. 43; no. 3; p. 267–270; Data Repository item 2015097 | doi:10.1130/G36386.1 | Published online 5 February 2015

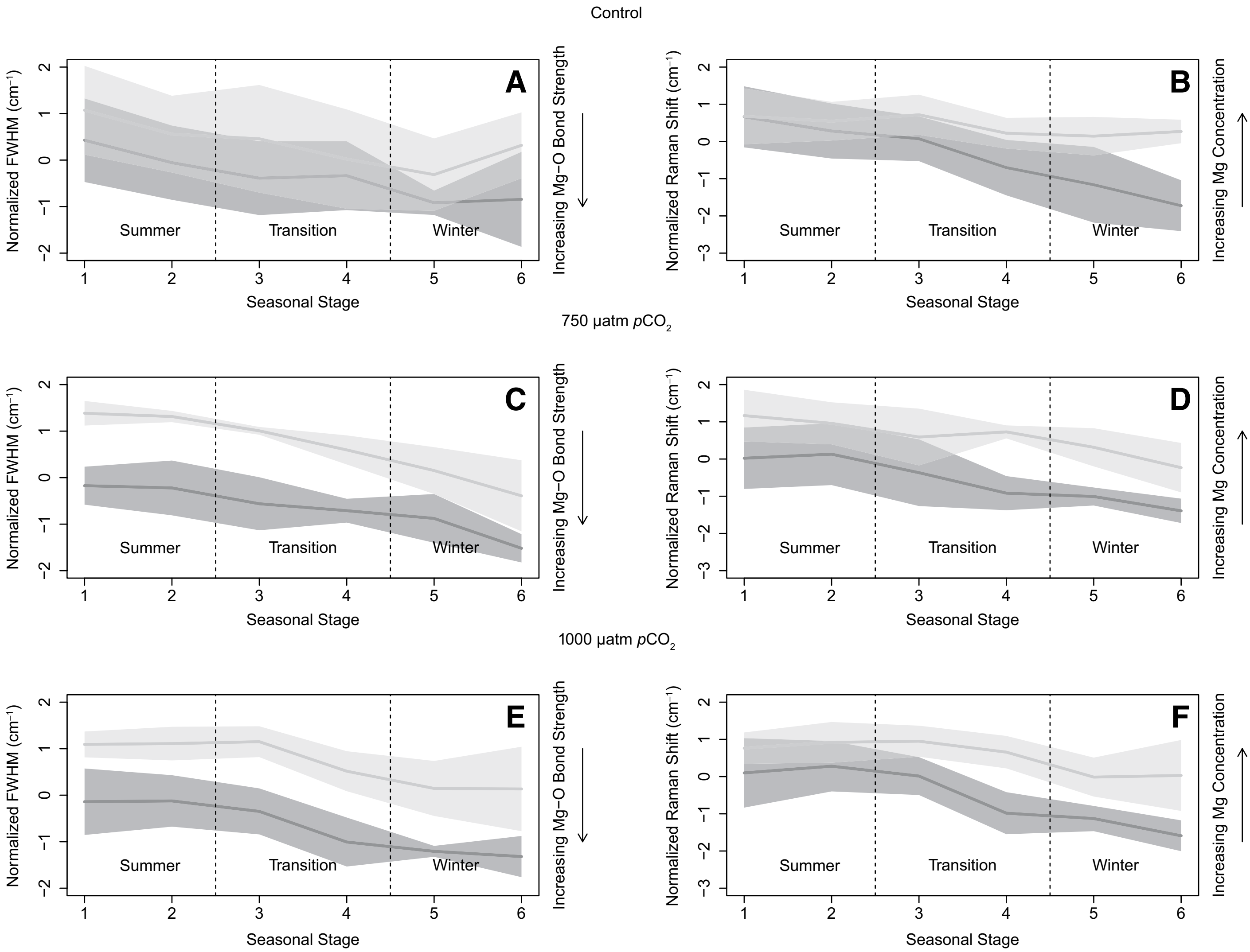

Figure 3. Average full width at half peak maximum (FWHM), indicative of Mg^{2+} positional disorder, Mg-O bond strength, and Mg concentrations. A–B: Control treatment average FWHM (A) and Mg concentrations (B). C–D: 750 µatm pCO_2 average FWHM (C) and Mg concentrations (D). E–F: 1000 µatm pCO_2 average FWHM (E) and Mg concentrations (F). Light gray line represents growth pre-treatment, dark gray line represents growth during treatment. Shaded area indicates standard deviation. Seasonal stages 1–2 represent summer, 5–6 winter, and 3–4 transition.

in the direction of the *c*-axis (Fig. DR1 in the GSA Data Repository[1]) (Bischoff et al., 1985). Thus reduced FWHM is caused by increased positional disorder, which in turn caused stronger Mg-O bonds. For full methods, see the Data Repository.

RESULTS

Seasonal Variability

Lithothamnion glaciale exhibited seasonal variation in skeletal parameters. Relative Mg concentrations were higher in summer while Mg-O bond strengths were weaker. Both parameters gradually declined and increased respectively across the seasonal transition into winter (Fig. 3).

Influence of pCO_2 on Structural Properties

While relative Mg concentrations were lower in all treatments after laboratory incubation (Fig. 3), a significant difference occurred only in the 1000 µatm pCO_2 treatment ($F = 21.96$, $df = 1$ [degrees of freedom], $p < 0.001$). The control treatment exhibited a significant relationship between relative Mg concentrations and seasonal stage (Fig. 3) ($F = 3.39$, $df = 1$, $p = 0.02$). This relationship was present, but non-significant, in the pCO_2 enrichment treatments (750 µatm: $F = 1.29$, $df = 5$, $p = 0.304$; 1000 µatm: $F = 1.03$, $df = 5$, $p = 0.425$). Bond strengths were higher in all treatments following incubation (Fig. 3), but with significant differences occurring only in the pCO_2 enrichment treatments (380 µatm: $F = 0.68$, $df = 1$, $p = 0.420$; 750 µatm: $F = 9.65$, $df = 1$, $p < 0.01$; 1000 µatm: $F = 18.65$, $df = 1$, $p < 0.01$).

Relationship Between *p*CO2 and Mg-O Bond Strength

There was a negative relationship between pCO_2 and FWHM when allowing for seasonally driven Mg concentrations present within the algae (Table 1; Fig. 4; Fig. DR2).

DISCUSSION

Mg-O bond strength within the high-Mg calcite skeleton of the coralline alga *L. glaciale* increases with increasing marine pCO_2 concentrations; this forms the basis for its utility as a pCO_2 proxy. While pCO_2 and other carbonate chemistry parameters can co-vary, pCO_2 was used to control the experimental carbonate chemistry and was the most stable carbonate parameter, so it was deemed to be the forcing

[1]GSA Data Repository item 2015097, full methods and carbonate chemistry, is available online at www.geosociety.org/pubs/ft2015.htm, or on request from editing@geosociety.org or Documents Secretary, GSA, P.O. Box 9140, Boulder, CO 80301, USA.

TABLE 1. pCO_2-FWHM RELATIONSHIP, WITH ASSOCIATED R^2 VALUE, STANDARD ERRORS (SE) ON INTERCEPT AND GRADIENT, AND *F* AND *p* STATISTICS

Relationship	R^2	Intercept SE	Gradient SE	*F*	*p*	pCO_2 FWHM^{-1}
FWHM (cm^{-1}) = –835 – (0.000521 × pCO_2) + (0.7678 × Mg [cm^{-1}])	0.32	140.30	0.00025	20.2	<0.001	87.9 µatm

Note: FWHM—normalized full width at half peak maximum (indicative of positional disorder and Mg-O bond strength). Mg—frequency of 1089 cm^{-1} Raman shift peak (positively correlated with Mg concentration and water temperature). Raw data used to determine the relationship are in Fig. 4 where they have not been adjusted for Mg. Once adjusted for Mg, pCO_2 has a ±28 µatm SE.

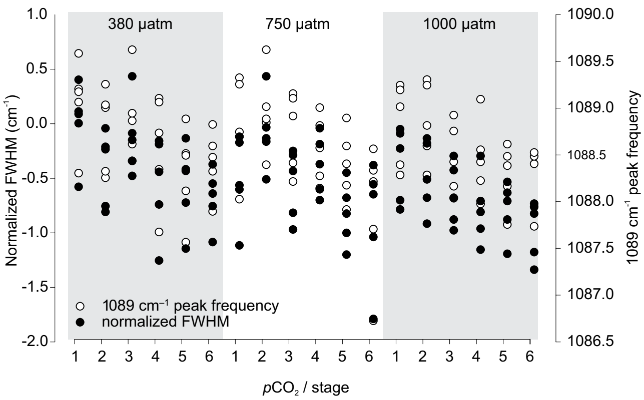

Figure 4. Normalized full width at half peak maximum (FWHM) in all *Lithothamnion glaciale* algae for each temporal stage at 380, 750, and 1000 µatm pCO_2 (alternating shaded and unshaded areas). FWHM is not adjusted for Mg concentration (see Fig. DR2 [see footnote 1] for Mg-adjusted data). Seasonal stages: 1–2 are summer, 3–4 are transition, 5–6 are winter.

factor driving changes in Mg-O bond strength. pCO_2 acts on coralline algae via HCO_3^- in the carbonate chemistry system; HCO_3^- is used as the substrate for calcification and as a carbon supplier during photosynthesis (Digby, 1977; Johnson et al., 2014; Koch et al., 2013).

Natural Seasonal Variability

Coralline algae show natural seasonal variability in Mg-O bond strength, with lower strengths present during summer months across treatments (Fig. 3). Structurally, bond strength increases as a consequence of increased position disorder when Mg ions move out of the *a*-axis into the *c*-axis (Bischoff et al., 1985). Thus during summer, the skeleton exhibits the least positional disorder in the calcite lattice. This may be due to optimal summer light and temperature conditions required for photosynthesis (Ries et al., 2009), causing better-controlled skeletal deposition.

The seasonal change in Mg concentrations (Figs. 3 and 4) is due to a positive correlation between Mg concentration and in situ temperatures driven by the abiotic replacement of Ca^{2+} by Mg^{2+} ions within the calcite lattice at higher temperatures (Kamenos et al., 2009). For *L. glaciale*, this relationship has been confirmed using electron microprobe analysis at this collection location (Kamenos, 2010; Kamenos et al., 2008), in Canada (Halfar et al., 2000), and in Greenland (Kamenos et al., 2012). These seasonal patterns in positional disorder and Mg-O bond strength underline the importance of either comparing high-Mg calcite that was deposited at the same time of year for different pCO_2 treatments or allowing for the concentration of Mg present. Absence of significant differences in Mg concentration and Mg-O bond strength between growth pre-collection and during the control treatment are important as they exclude experimental handling impacts.

The Influence of pCO_2 on Coralline Algal Structure

At both 750 and 1000 µatm pCO_2, there was an increase in skeletal positional disorder and Mg-O bond strength in *L. glaciale* (Figs. 3 and 4). Although higher growth would be expected at high pCO_2 in photosynthesizers, red coralline algae dissolve at night under high pCO_2 and then hypercalcify during the day (Kamenos et al., 2013; Martin et al., 2013). Rapid hypercalcification likely leads to poor control over skeletal deposition resulting in greater positional disorder and thus Mg-O bond strength.

Despite their high-Mg calcite skeleton, a less stable polymorph of $CaCO_3$ than calcite or aragonite, coralline algae appear to lower their Mg content at higher pCO_2 (Fig. 3). This could be due to (1) preferential Mg^{2+} leaching, or (2) reduction of skeletally incorporated Mg^{2+} by the algae themselves, thereby reducing solubility and vulnerability to acidified conditions (Kamenos et al., 2013; Ries et al., 2009). Thus while hypercalcification to overcome dissolution indicates poor control over structural skeletal deposition, simultaneously reduced Mg $^{2+}$ content indicates either (1) increased active chemical control over their skeleton, or (2) reduced chemical skeletal control allowing Mg^{2+} leaching.

A single significant negative relationship between FWHM and pCO_2 exists across calcite deposited in all seasons when allowing for Mg concentrations with a ±28 µatm standard error on pCO_2 calculations (Table 1). Adjusting for Mg concentrations within the calcite skeleton is preferential to generation of season-specific relationships, as this (1) accounts for differences in inter-annual temperature causing a temporal offset in reconstructed pCO_2, and (2) minimizes variability introduced by the within-growth band location of each analysis.

Temporal Resolution

Six analytical sites per growth band were assessed in *L. glaciale*, fixing temporal sampling at two-month resolution. However, temperature reconstructions at two-week resolution are achievable from *L. glaciale* when using Mg paleothermometry (Kamenos et al., 2008). With suitable instrumental parameters, Raman laser spot size can be <10 µm indicating that pCO_2 reconstructions at two-week resolution may also be possible.

Proxy Temporal Stability

In addition to skeletal Mg^{2+} reduction, OA-induced Mg-O bond strength changes may be enhanced with secondary environmental stressors, including temperature. Any historic changes in temperature will also have changed skeletal Mg concentrations (Halfar et al., 2000, Kamenos et al., 2008). This in turn affects Mg-O bond strength (Bischoff et al., 1985), as shown here at a seasonal scale (Figs. 3 and 4), further reducing skeletal reactivity to reduced pH during winter. This stresses the importance of incorporating Mg concentrations in reconstructions using Mg-O bond strength (e.g., Table 1). Similarly, any season-specific differences in Mg concentrations between pre-experimental and experimental growth not attributed to the experimental treatment are likely due to subtle site-specific differences between in situ (pre-experimental growth) and experimental temperatures in successive years.

CONCLUSIONS

Red coralline algae show significant potential to act as pCO_2 proxies via use of their skeletal bonding strength. High-latitude species, including *L. glaciale*, are of particular importance in detecting historic changes in pCO_2 enrichment as these species may experience the first pCO_2 enrichment via OA due to high-latitude shoaling of the $\Omega_{Calcite}$ (saturation state) depth (Feely et al., 2004). Moreover, there is a paucity of high-latitude shallow-water OA proxies in comparison to developments being made with equatorial and deep-water proxies including corals and foraminifera. We determined relationships between pCO_2 and coralline algal skeletal Mg-O bond strength, a key step in understanding the capacity of molecular bonding strength to record pCO_2. Instrumental costs for Raman are modest, sample preparation is minimal, and analytical times are fast. This provides a tool for reconstructing paleo-pCO_2 which is not only a key carbonate chemistry parameter but also a critical parameter for understanding historic atmospheric CO_2 concentrations.

ACKNOWLEDGMENTS

We thank H. Stahl and N. Hicks for dissolved inorganic carbon analysis at the Scottish Association for Marine Science. Kamenos was funded by a Royal Society of Edinburgh Personal Research Fellowship (RES 48704/1) and Natural Environment Research Council (UK) grant NE/H017305/1. Pauly was funded by a Natural Sciences and Engineering Research Council of Canada Discovery Grant to E. LeDrew. Donohue was in receipt of a Marine Alliance for Science and Technology Ph.D. studentship. We thank the reviewers and editor (Ellen Thomas) whose comments improved the manuscript. This paper is a contribution to the UK Ocean Acidification Research Programme.

REFERENCES CITED

Adey, W.H., and McKibbin, D.L., 1970, Studies on maerl species *Phymatolithon calcareum* (Pallas) nov. comb. and *Lithothamnion coralloides* Crouan in the Ria de Vigo: Botanica Marina, v. 13, p. 100–106, doi:10.1515/botm.1970.13.2.100.

Babila, T.L., Rosenthal, Y., and Conte, M.H., 2014, Evaluation of the biogeochemical controls on B/Ca of *Globigerinoides ruber* white from the Oceanic Flux Program, Bermuda: Earth and Planetary Science Letters, v. 404, p. 67–76, doi:10.1016/j.epsl.2014.05.053.

Bates, N.R., Best, M.H.P., Neely, K., Garley, R., Dickson, A.G., and Johnson, R.J., 2012, Detecting anthropogenic carbon dioxide uptake and ocean acidification in the North Atlantic Ocean: Biogeosciences, v. 9, p. 2509–2522, doi:10.5194/bg-9-2509-2012.

Bischoff, W.D., Sharma, S.K., and Mackenzie, F.T., 1985, Carbonate ion disorder in synthetic and biogenic magnesian calcites: A Raman spectral study: The American Mineralogist, v. 70, p. 581–589.

Burdett, H., 2014, Climate change ecology: Older and wiser: Nature Climate Change, v. 4, p. 668–669, doi:10.1038/nclimate2316.

Digby, P.S.B., 1977, Growth and calcification in coralline algae, *Clathromorphum circumscriptum* and *Corallina officinalis*, and significance of pH in relation to precipitation: Journal of the Marine Biological Association of the United Kingdom, v. 57, p. 1095–1109, doi:10.1017/S0025315400026151.

Doney, S.C., Fabry, V.J., Feely, R.A., and Kleypas, J.A., 2009, Ocean acidification: The other CO_2 problem: Annual Review of Marine Science, v. 1, p. 169–192, doi:10.1146/annurev.marine.010908.163834.

Dupont, S., and Portner, H.O., 2013, A snapshot of ocean acidification research: Marine Biology, v. 160, p. 1765–1771, doi:10.1007/s00227-013-2282-9.

Fabricius, K.E., Langdon, C., Uthicke, S., Humphrey, C., Noonan, S., De'ath, G., Okazaki, R., Muehllehner, N., Glas, M.S., and Lough, J.M., 2011, Losers and winners in coral reefs acclimatized to elevated carbon dioxide concentrations: Nature Climate Change, v. 1, p. 165–169, doi:10.1038/nclimate1122.

Feely, R.A., Sabine, C.L., Lee, K., Berelson, W., Kleypas, J., Fabry, V.J., and Millero, F.J., 2004, Impact of anthropogenic CO_2 on the $CaCO_3$ system in the oceans: Science, v. 305, p. 362–366, doi:10.1126/science.1097329.

Foster, G.L., Lear, C.H., and Rae, J.W.B., 2012, The evolution of $pCO_{(2)}$, ice volume and climate during the middle Miocene: Earth and Planetary Science Letters, v. 341–344, p. 243–254, doi:10.1016/j.epsl.2012.06.007.

Foster, G.L., Honisch, B., Paris, G., Dwyer, G.S., Rae, J.W.B., Elliott, T., Gaillardet, J., Hemming, N.G., Louvat, P., and Vengosh, A., 2013, Interlaboratory comparison of boron isotope analyses of boric acid, seawater and marine $CaCO_3$ by MC-ICPMS and NTIMS: Chemical Geology, v. 358, p. 1–14, doi:10.1016/j.chemgeo.2013.08.027.

Foster, M.S., 2001, Rhodoliths: Between rocks and soft places: Journal of Phycology, v. 37, p. 659–667, doi:10.1046/j.1529-8817.2001.00195.x.

Halfar, J., Zack, T., Kronz, A., and Zachos, J. C., 2000, Growth and high-resolution paleoenvironmental signals of rhodoliths (coralline red algae): A new biogenic archive: Journal of Geophysical Research, v. 105, p. 22,107–22,116, doi:10.1029/1999JC000128.

Hall-Spencer, J.M., Rodolfo-Metalpa, R., Martin, S., Ransome, E., Fine, M., Turner, S.M., Rowley, S.J., Tedesco, D., and Buia, M.C., 2008a, Volcanic carbon dioxide vents show ecosystem effects of ocean acidification: Nature, v. 454, p. 96–99, doi:10.1038/nature07051.

Hall-Spencer, J.M., Rofolfo-Metalpa, R., Martin, S., Ransome, E., Fine, M., Turner, S.M., Rowley, S.J., Tedesco, D., and Buia, M.-C., 2008b, Volcanic carbon dioxide vents show ecosystem effects of ocean acidification: Nature, v. 454, p. 96–99, doi:10.1038/nature07051.

Henehan, M.J., et al., 2013, Calibration of the boron isotope proxy in the planktonic foraminifera *Globigerinoides ruber* for use in palaeo-CO_2 reconstruction: Earth and Planetary Science Letters, v. 364, p. 111–122, doi:10.1016/j.epsl.2012.12.029.

Henrich, R., Freiwald, A., Betzler, C., Bader, B., Schafer, P., Samtleben, C., Brachert, T.C., Wehrmann, A., Zankl, H., and Kuhlmann, D.H.H., 1995, Controls on modern carbonate sedimentation on warm-temperature to Arctic coasts, shelves and seamounts in the Northern Hemisphere: Implications for fossil counterparts: Facies, v. 32, p. 71–108, doi:10.1007/BF02536865.

Honisch, B., et al., 2012, The geological record of ocean acidification: Science, v. 335, p. 1058–1063, doi:10.1126/science.1208277.

Inoue, S., Kayanne, H., Yamamoto, S., and Kurihara, H., 2013, Spatial community shift from hard to soft corals in acidified water: Nature Climate Change, v. 3, p. 683–687, doi:10.1038/nclimate1855.

Johnson, M.D., Moriarty, V.W., and Carpenter, R.C., 2014, Acclimatization of the crustose coralline alga *Porolithon onkodes* to variable $pCO_{(2)}$: PLoS ONE, v. 9, e87678, doi:10.1371/journal.pone.0087678.

Kamenos, N.A., 2010, North Atlantic summers have warmed more than winters since 1353, and the response of marine zooplankton: Proceedings of the National Academy of Sciences of the United States of America, v. 107, p. 22,442–22,447, doi:10.1073/pnas.1006141107.

Kamenos, N.A., Cusack, M., and Moore, P.G., 2008, Coralline algae are global palaeothermometers with bi-weekly resolution: Geochimica et Cosmochimica Acta, v. 72, p. 771–779, doi:10.1016/j.gca.2007.11.019.

Kamenos, N.A., Cusack, M., Huthwelker, T., Lagarde, P., and Scheibling, R.E., 2009, Mg-lattice associations in red coralline algae: Geochimica et Cosmochimica Acta, v. 73, p. 1901–1907, doi:10.1016/j.gca.2009.01.010.

Kamenos, N.A., Hoey, T., Nienow, P., Fallick, A.E., and Claverie, T., 2012, Reconstructing Greenland ice sheet runoff using coralline algae: Geology, v. 40, p. 1095–1098, doi:10.1130/G33405.1.

Kamenos, N.A., Burdett, H.L., Aloisio, E., Findlay, H.S., Martin, S., Longbone, C., Dunn, J., Widdicombe, S., and Calosi, P., 2013, Coralline algal structure is more sensitive to rate, rather than the magnitude, of ocean acidification: Global Change Biology, v. 19, p. 3621–3628, doi:10.1111/gcb.12351.

Keeling, C.D., and Whorf, T.P., 1999, Atmospheric CO_2 records from sites in the SIO air sampling network, *in* Trends: A Compendium of Data on Global Change: Oak Ridge, Tennessee, Carbon Dioxide Information Analysis Center, Oak Ridge National Laboratory: http://cdiac.ornl.gov/trends/co2/sio-keel.html (January 2014).

Koch, M., Bowes, G., Ross, C., and Zhang, X.-H., 2013, Climate change and ocean acidification effects on seagrasses and marine macroalgae: Global Change Biology, v. 19, p. 103–132, doi:10.1111/j.1365-2486.2012.02791.x.

Kuffner, I.B., Andersson, A.J., Jokiel, P.L., Rodgers, K.S., and Mackenzie, F.T., 2007, Decreased abundance of crustose coralline algae due to ocean acidification: Nature Geoscience, v. 1, p. 114–117, doi:10.1038/ngeo100.

Martin, S., Cohu, S., Vignot, C., Zimmerman, G., and Gattuso, J.P., 2013, One-year experiment on the physiological response of the Mediterranean crustose coralline alga, *Lithophyllum cabiochae*, to elevated pCO_2 and temperature: Ecology and Evolution, v. 3, p. 676–693, doi:10.1002/ece3.475.

McCoy, S.J., and Ragazzola, F., 2014, Skeletal trade-offs in coralline algae in response to ocean acidification: Nature Climate Change, v. 4, p. 719–723, doi:10.1038/nclimate2273.

Nash, M.C., et al., 2013, Dolomite-rich coralline algae in reefs resist dissolution in acidified conditions: Nature Climate Change, v. 3, p. 268–272, doi:10.1038/nclimate1760.

Penman, D.E., Honisch, B., Zeebe, R.E., Thomas, E., and Zachos, J.C., 2014, Rapid and sustained surface ocean acidification during the Paleocene-Eocene Thermal Maximum: Paleoceanography, v. 29, p. 357–369, doi:10.1002/2014PA002621.

Ries, J.B., Cohen, A.L., and McCorkle, D.C., 2009, Marine calcifiers exhibit mixed responses to CO_2-induced ocean acidification: Geology, v. 37, p. 1131–1134, doi:10.1130/G30210A.1.

Roleda, M.Y., Boyd, P.W., and Hurd, C.L., 2012, Before ocean acidification: Calcifier chemistry lessons: Journal of Phycology, v. 48, p. 840–843, doi:10.1111/j.1529-8817.2012.01195.x.

Tans, P., 2014, Trends in Atmospheric Carbon Dioxide: Boulder, Colorado, National Oceanic and Atmospheric Administration Earth System Research Laboratory, http://www.esrl.noaa.gov/gmd/ccgg/trends/ (accessed April 2014).

Zachos, J.C., et al., 2005, Rapid acidification of the ocean during the Paleocene-Eocene thermal maximum: Science, v. 308, p. 1611–1615, doi:10.1126/science.1109004.

Manuscript received 23 October 2014
Revised manuscript received 9 January 2015
Manuscript accepted 22 January 2015

Printed in USA